Vibrational energy relaxation of benzene dimer and trimer in the CH stretching region studied by picosecond time-resolved IR-UV pump-probe spectroscopy

Ryoji Kusaka, Yoshiya Inokuchi, and Takayuki Ebata

Citation: J. Chem. Phys. **136**, 044304 (2012); doi: 10.1063/1.3676658
View online: http://dx.doi.org/10.1063/1.3676658
View Table of Contents: http://jcp.aip.org/resource/1/JCPSA6/v136/i4
Published by the American Institute of Physics.

Vibrational energy relaxation of benzene dimer and trimer in the CH stretching region studied by picosecond time-resolved IR-UV pump-probe spectroscopy

Ryoji Kusaka, Yoshiya Inokuchi, and Takayuki Ebata[a)]
Department of Chemistry, Graduate School of Science, Hiroshima University, Higashi-Hiroshima 739-8526, Japan

(Received 12 October 2011; accepted 20 December 2011; published online 23 January 2012)

Vibrational energy relaxation (VER) of the Fermi polyads in the CH stretching vibration of the benzene dimer (Bz_2) and trimer (Bz_3) has been investigated by picosecond (ps) time-resolved IR-UV pump-probe spectroscopy in a supersonic beam. The vibrational bands in the 3000–3100 cm^{-1} region were excited by a ps IR pulse and the time evolutions at the pumped and redistributed (bath) levels were probed by resonance enhanced multiphoton ionization with a ps UV pulse. For Bz_2, a site-selective excitation in the T-shaped structure was achieved by using the isotope-substituted heterodimer *hd*, where $h = C_6H_6$ and $d = C_6D_6$, and its result was compared with that of *hh* homodimer. In the *hd* heterodimer, the two isomers, *h*(stem)*d*(top) and *h*(top)*d*(stem), show remarkable site-dependence of the lifetime of intracluster vibrational energy redistribution (IVR); the lifetime of the Stem site [*h*(stem)*d*(top), 140–170 ps] is ~2.5 times shorter than that of the Top site [*h*(top)*d*(stem), 370–400 ps]. In the transient UV spectra, a broad electronic transition due to the bath modes emerges and gradually decays with a nanosecond time scale. The broad transition shows different time profile depending on UV frequency monitored. These time profiles are described by a three-step VER model involving IVR and vibrational predissociation: initial → bath1(intramolecular) → bath2(intermolecular) → fragments. This model also describes well the observed time profile of the Bz fragment. The *hh* homodimer shows the stepwise VER process with time constants similar to those of the *hd* dimer, suggesting that the excitation-exchange coupling of the vibrations between the two sites is very weak. Bz_3 also exhibited the stepwise VER process, though each step is faster than Bz_2. © *2012 American Institute of Physics*. [doi:10.1063/1.3676658]

I. INTRODUCTION

Benzene clusters have been of special interest as a prototypical example of molecular clusters formed by an aromatic-aromatic force field. The interaction in such π-systems often plays a crucial role in the self-assembly of biomolecular systems.[1–7] Among them, benzene dimer (Bz_2) has been extensively studied experimentally[8–26] and theoretically.[27–54] Many of these studies have been devoted to the determination of the most stable structure: particularly T-shaped or parallel-displaced (PD) structure. Many of the experimental studies, molecular-beam electric deflection,[8,9] UV-UV hole-burning spectroscopy,[21] and Raman-UV double resonance spectroscopy[22] suggest that the two benzene molecules are not symmetrically equivalent to each other. The rotational constant obtained by the Fourier-transform microwave spectrum[23] indicates the T-shaped structure. In addition to the experiments, quantum chemical calculations (e.g., Ref. 54) suggested that a tilted T-shaped structure is the global minimum, although many isomers, including the PD isomer, exist in almost isoenergetic region. From these studies, it is generally accepted that the global minimum of Bz_2 is the floppy T-shaped structure.

In addition to the structure, vibrational energy relaxation (VER) is also an important subject for benzene clusters since the VER dynamics is intimately related to the structure. In the T-shaped Bz_2, two benzene molecules are at different symmetrical positions, so that the "intramolecular mode ↔ bath mode" anharmonic coupling will be different between the two sites and the dimer will show the VER dynamics characteristic of each site. Several studies on VER of benzene clusters in S_0 have been reported.[55–57] Lee and co-workers[55,57] and Fischer[56] estimated the lifetime (τ) of the CH stretching energy region to be in the range of 10^{-12} s $< \tau < 10^{-11}$ s, based on the bandwidth measurement of the IR band. Felker and coworkers reported that the ν_2 (CH stretching, Wilson's numbering) level of the Stem site relaxes faster than that of the Top site, from the difference of the widths of Raman bands.[22] In both cases, however, the measured bandwidth is the sum of many rovibrational levels, so that one cannot exclude the contribution of inhomogeneous width. Moreover, it is not clear how the bandwidth is related to the dynamics of VER, such as intramolecular (intracluster) vibrational energy redistribution (IVR) and vibrational predissociation (VP). Thus, the time-resolved spectroscopic study is essential to fully understand VER of Bz_2.

In our previous study,[58] we investigated the first step of VER of Bz_2 by picosecond IR-UV pump-probe spectroscopy in a supersonic beam. In order to achieve site-selective

a)Author to whom corresponding should be addressed. Electronic mail: tebata@hiroshima-u.a.cjp.

vibrational excitation of the T-shaped Bz_2, we used the *hd* dimer ($h = C_6H_6$, $d = C_6D_6$). This dimer has two isomers, *h*(stem)*d*(top) and *h*(top)*d*(stem), which coexist almost equally in the supersonic beam. After the IR pulse excitation of one of the Fermi polyads in the CH stretching region (3077 cm^{-1}), the decay profiles of the initial levels were observed by (1 + 1) resonance enhanced multiphoton ionization (REMPI) with a UV laser pulse for each isotopomer. We reported that the IVR decay lifetime showed a remarkable site-dependence; the Stem site [*h*(stem)*d*(top), 110 ps] decays 4.5 times faster than the Top site [*h*(top)*d*(stem), 500 ps], in spite of very small energy difference ($\sim$1 cm^{-1}) between the two vibrational levels.[25] In addition, we reported the appearance of a broad electronic transition of the redistributed levels (bath modes).

In the present paper, we report (1) a detailed time-resolved study of the *hd* dimer to give whole view of VER, (2) VER of the *hh* homodimer to extract information about the coupling of the vibrations between the two sites in the *hh* dimer, and (3) VER of larger size cluster, benzene trimer (Bz_3), to investigate the size effect.

II. EXPERIMENTAL AND ANALYSIS

The experimental setup of the picosecond time-resolved IR-UV pump-probe spectroscopy is an upgraded version of that described in our previous papers.[58–63] Briefly, a picosecond IR pulse laser is obtained by difference frequency generation (DFG) between 1.064 μm and an idler output of an optical parametric generation/optical parametric amplifier (OPG/OPA) system (Ekspra PG401/DFG2-10P) pumped by a mode-locked picosecond Nd:YAG laser (Ekspra PL2143S). A picosecond UV pulse laser is obtained by second harmonic generation of the output of another OPG/OPA (Ekspra PG401SH) system pumped by the same Nd:YAG laser. The spectral resolution of the IR and UV lights are 5 cm^{-1}, and the time resolution of the two pulses is 12 ps. The delay time between the IR and UV pulses is changed by an optical delay line. In the present study, a gaseous mixture of C_6H_6 and C_6D_6 [50:50(v/v)] diluted with helium carrier gas at a total pressure of 3 bar is expanded into vacuum by a pulsed valve (General valve, Series 9). The molecular beam is obtained by skimming the center of the expansion. To reduce the formation of larger size clusters, a container of the sample is maintained at -20°C, and the width and timing of the pulsed valve is carefully controlled. The IR and UV laser lights cross the molecular beam with a counter propagating geometry. The generated ions are mass-analyzed by a time-of-flight mass spectrometer and detected by a channeltron (Burle 4900). The ion signals are processed by a boxcar integrator (Par model 4401/4420) connected by a personal computer.

Figure 1 shows an energy level diagram of Bz_2 and a pump-probe excitation scheme. A picosecond IR pulse excites Bz_2 to one of the Fermi-polyads in the CH stretch region, and the excited level is monitored by (1 + 1) REMPI with a picosecond UV pulse. The time evolution of the population is observed by changing the delay time (Δt) between IR and UV pulses. The UV energy and the mass of the ion monitored are properly chosen for the selective measurements of the pumped and bath levels of the parent and fragment species. The obtained time profiles are analyzed by using the VER model with two bath modes as shown in Fig. 1. The validity of this model is described in Sec. III D 1.

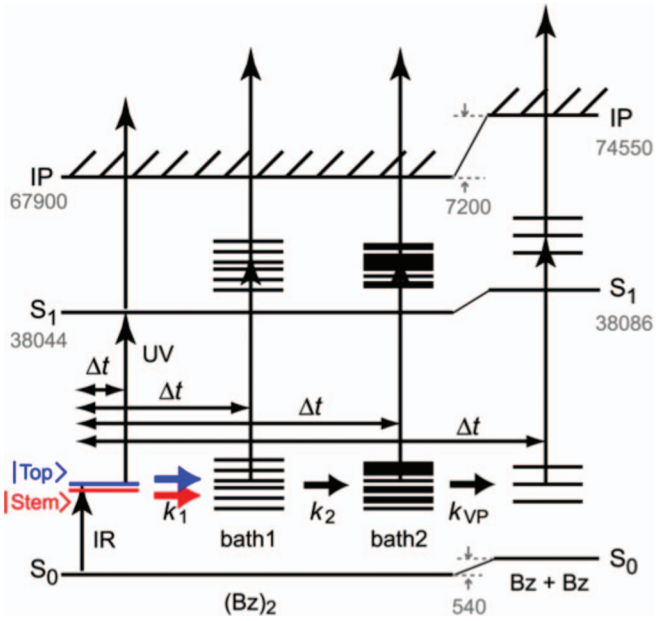

FIG. 1. Schematic energy level diagram in VER of Bz_2 and a pump-probe excitation scheme. In this figure, energy difference between S_0, S_1, and IP for $(Bz)_2$ and Bz as well as the dissociation energy in neutral and ionic states are embedded with cm^{-1} unit. The values are taken from Ref. 67.

III. RESULTS AND DISCUSSION

A. IR spectra of Bz_2

Figure 2(a) shows an IR spectrum of benzene monomer in the CH stretching region measured by a nanosecond laser

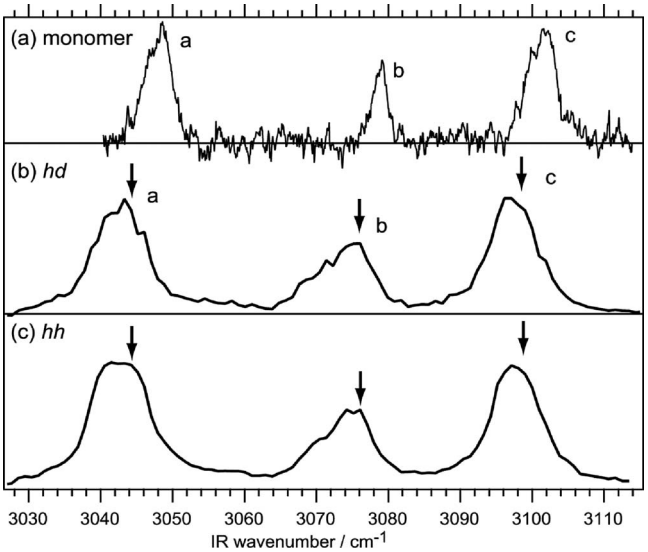

FIG. 2. (a): IR spectrum of benzene monomer measured by a nanosecond laser system. (b)-(c): IR spectra obtained by monitoring hd^+ and hh^+ mass channels, respectively, with a picosecond laser system. Arrows show the IR excitation energy used for the pump-probe experiment.

system. This spectrum is obtained as a dip spectrum by IR-UV double resonance spectroscopy and is shown in an inverted manner. The appearance of three bands (bands **a**, **b**, and **c**) is due to the Fermi resonance between the IR-active CH stretching level (ν_{20}) and the $\nu_8+\nu_{19}$ and $\nu_1+\nu_6+\nu_{19}$ combination levels, where each component is the in-plane vibration of benzene monomer.[64] Figures 2(b) and 2(c) display the ion-gain IR spectra of Bz_2 by monitoring the hd^+ and hh^+ mass signals, respectively. These spectra were observed by the picosecond laser system at $\Delta t = 300$ ps with ν_{UV} fixed at the broad transition in the transient spectrum (37 600 cm^{-1}). The IR spectra of the *hd* and *hh* dimers are quite similar to each other though the positions of the three bands are 2–4 cm^{-1} redshifted compared to those of the monomer bands.

It should be noted that each polyad in the *hd* and *hh* dimers contains two vibrational levels due to the Stem and Top components. The energy interval between the two levels are ~1 cm^{-1}.[25] Thus, simultaneous excitation of both levels by the ps IR pulse laser is unavoidable. This situation provides different conditions for the *hd* and *hh* dimers. In the *hd* dimer, two vibrationally excited isomers, *h**(stem)*d*(top) and *h**(top)*d*(stem), are simultaneously generated by the excitation, while the two vibrational levels are coherently excited in the *hh* homodimer. The comparison between the decay profiles of the *hd* and *hh* dimers provides important information on the coupling of the vibrations between the two sites of Bz_2, as discussed later.

B. Transient UV spectra of Bz_2 after the IR excitation of Fermi-polyad

Figure 3 shows the transient (1 + 1) REMPI spectra obtained by monitoring (a) hd^+ and (b) hh^+ mass channels after the IR excitation of bands **a**, **b**, and **c**. These spectra were observed at three different delay times: (black) +30 ps, (red) +100 ps, and (blue) +300 ps. Also shown are the (1 + 1) REMPI spectra without IR excitation (green). The right panel shows the (1 + 1) REMPI spectra in the band origin region. In Fig. 3(c), the UV laser power is plotted. The transient spectra show similar features between the *hd* and *hh* dimers: the sharp bands at ~36 400, ~36 950, and ~37 400 cm^{-1}, and the structureless broad band in wide energy region. With an increase of the delay time, the sharp bands disappear while the broad band emerges. The sharp bands at ~36 400, ~36 950, and ~37 400 cm^{-1} are due to the vibronic transitions from the pumped levels, which correspond to the transitions to the 19^1, 6^119^1, and 6^219^1 levels, respectively.[58] The broad band is assigned to overlapped transitions of the redistributed (bath) levels. In the spectra of band **a** excitation, the sharp bands are not seen and the broad band is prominent. This is because of small coefficients of modes ν_6 and ν_{19} for the state of band **a**.[64]

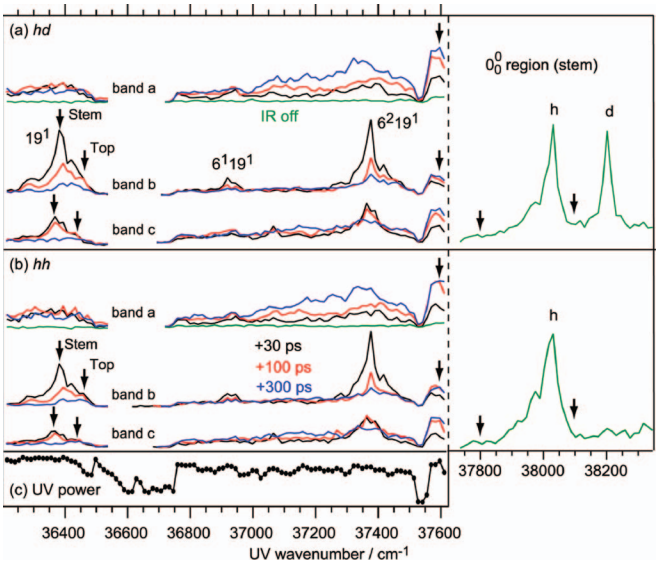

FIG. 3. Transient UV spectra at $\Delta t = +30$ (black), +100 (red), and +300 ps (blue) observed with the IR excitations fixed at each Fermi band (bands **a**, **b**, and **c**). Green ones are UV spectra measured without IR excitation. The UV spectra (a) and (b) are obtained by monitoring hd^+ and hh^+ mass channels, respectively. In panel (c), UV power is plotted. Arrows show the UV energy used for the observation of time profiles.

As described above, the vibrational energies of the Stem and Top sites of the T-shaped Bz_2 differ by only ~1 cm^{-1}, so that two isomers of the *hd* dimer are simultaneously excited, while the two levels are coherently excited in the *hh* dimer by a picosecond IR pulse. Thus, the transient spectra of Fig. 3 involve the transitions of the Stem and Top sites of Bz_2. In the (1 + 1) REMPI spectrum of Bz_2 observed by a nanosecond laser,[21,22] the Stem site exhibits a sharp vibronic band, while the Top site exhibits a progression of ~15 cm^{-1} interval in the higher-energy region of the sharp band of the Stem site Bz. Similarly, in Fig. 3, each band at ~36 400, ~36 950 and ~37 400 cm^{-1} contains the Stem and Top transitions. In each band, the progression of the Top site is not resolved, and shows a broad feature with the peak at ~50 cm^{-1} higher energy side of the Stem band.[58] We observed decay time profiles by monitoring the band $CH^0{}_119^1{}_0$ at ν_{UV} = ~36 400 cm^{-1}. The probed positions are marked by arrows in Fig. 3.

C. IVR of the IR-pumped levels of Bz_2

1. IVR decay of hd and hh dimers

Figure 4 shows the decay time profiles of the *hd* and *hh* dimers after the IR excitation of bands **b** and **c**. Each panel shows the decay profiles observed by monitoring the Stem (upper) and Top (lower) site transitions. The time profiles can be fitted by the single-exponential decay and its convolution with Gaussian function pulse of 12 ps FWHM (red curves). The obtained lifetimes are shown in the figure and listed in Table I. For the decay profiles of the *hd* dimer with the band **b** excitation [Fig. 4(a)], we reported that the lifetimes of the Stem and Top sites were 110 ps and 500 ps, respectively, in our previous paper.[58] However, in the present study, we obtained slightly different values: 140 ps for the Stem site and 370 ps for the Top site. The discrepancy is ascribed to the improved alignment of the optical delay line and careful check of extra signals coming from the fragmentation of larger clusters. Thus, we believe that the time constants of the present study are more reliable than those of the previous work.

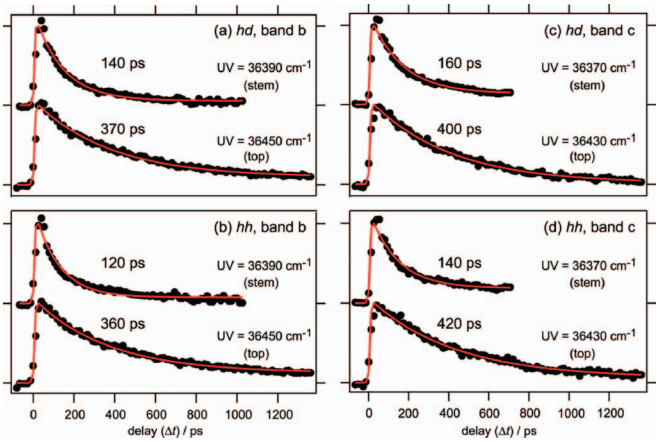

FIG. 4. Decay time profiles measured by monitoring hd^+ and hh^+ mass channels after the IR excitation at bands **b** and **c**. Two decay profiles in each panel were observed at different probe UV frequencies. Red curves correspond to the single-exponential decay function convoluted with the IR and UV Gaussian pulses. The best decay lifetimes are embedded in this figure.

In the IVR decay profiles in Fig. 4, three characteristics can be seen for the IVR of the *hd* and *hh* dimers. (1) In both species, IVR of the Stem site occurs 2.5–3 times faster than that of the Top site. (2) The IVR lifetimes are almost independent of the IR bands. (3) There is almost no difference in the decay profiles between the *hd* and *hh* dimers. These findings provide us with following information about the coupling of the vibrations in Bz_2. First, (1) the anharmonic coupling strength between a Fermi polyad and bath modes is stronger at the Stem site than at the Top site. Second, (2) the anharmonic coupling strength between a Fermi polyad and bath modes is almost the same among the three Fermi polyads. Third, (3) the excitation-exchange coupling between the two stationary states of the Stem and Top site Bz molecules is very weak even in the *hh* dimer. In our previous paper,[58] we already discussed the reasons of (1) and (2). As to (1), we proposed that the lower symmetrical environment and the in-plane vibrational motion of the Stem site Bz facilitate the effective coupling with bath modes. As to (2), each polyad state is constructed by essentially the same zeroth-order vibrational modes through the Fermi resonance, leading to similar property for IVR. In Sec. III C 2, we will discuss the reason of (3).

Here, we compare the IVR lifetime of Bz_2 in S_0 obtained in this work with those previously reported. As was described in the Introduction, Lee and co-workers[55,57] and Fischer[56] estimated the lifetime of ν_{20} to be in the range of 1–10 ps by the bandwidth in the IR spectra, where they did not specify the lifetime of the Stem and Top sites. Felker and co-workers[22] reported that the lifetime of ν_2 of the Stem site is 18 ps, and that of Top site is larger than that of Stem site, which were estimated by ionization loss stimulated Raman-UV double resonance spectra. These previous studies reported much shorter lifetime than those of the present work. One of the reasons why the bandwidth measurement gave the shorter lifetime is that the widths involve the inhomogeneous broadening due to many rotational lines because these experiments monitor many rotational lines of the clusters even under the jet-cooled condition. However, the lifetime estimated by bandwidth of the Raman bands is probable because the Raman active ν_2 band mostly contains Q-branch. If the difference of the IVR lifetime between ν_2 and ν_{20} is true, this result indicates the mode selectivity of IVR rate constants. In this sense, a time-resolved picosecond Raman-UV pump-probe experiment will be necessary to confirm the faster IVR rate constant.

2. Excitation-exchange coupling between Stem and Top sites of the hh dimer

As described above, the *hh* [*h*(stem)*h*(top)] dimer has two nearly degenerated vibrational levels with the energy difference of $\sim$1 cm^{-1} and they are coherently excited by a picosecond IR pulse. The energy gap of $\sim$1 cm^{-1} will lead to a quantum beat with roughly 30 ps period in the decay profiles of the *hh* dimer. We previously observed quantum beat of deuterated phenol having a similar energy gap (0.7 cm^{-1}),[61] by using the same picosecond laser system. Thus, it is possible to observe the quantum beat of the *hh* dimer. However, in Figs. 4(b) and 4(d), both of Stem and Top sites in the *hh* dimer show a single-exponential decay and their time constants are very similar to those of the *hd* dimer. The lack of the quantum beat in spite of the coherent vibrational excitation of *hh* homodimer indicates a negligible excitation-exchange coupling between the vibrations of the Stem and Top sites, which is discussed in supplementary material.[65] A similar conclusion was also given for ν_2 CH-stretch excitation of the *hh* dimer by frequency-resolved Raman results.[22] This negligibly small coupling strength between the Stem and Top sites can be supported by the motions of the CH stretching vibrations of the T-shaped Bz_2 calculated by quantum chemical calculation. The tilted T-shaped geometry (C_s symmetry) was optimized

TABLE I. Time constants (ps) on vibrational energy relaxation of benzene dimer and trimer after the IR excitation of the Fermi polyads (band **a** **b**, and **c**) of the CH stretching vibration.

	Band a		Band b		Band c		
	hd	*hh*	*hd*	*hh*	*hd*	*hh*	*hdd*
τ_1(ps) stem	…[a]	…[a]	140 ± 10	120 ± 10	160 ± 10	140 ± 10	50 ± 10[b]
top	…[a]	…[a]	370 ± 20	360 ± 20	400 ± 20	420 ± 30	
τ_2(ps)			200–700				300 ± 100[b]
τ_{vp}(ps)			2000–6000				1000 ± 200[b]

[a]Decay time profiles cannot be observed.
[b]Determined from time profiles observed by monitoring dd^+ signal.

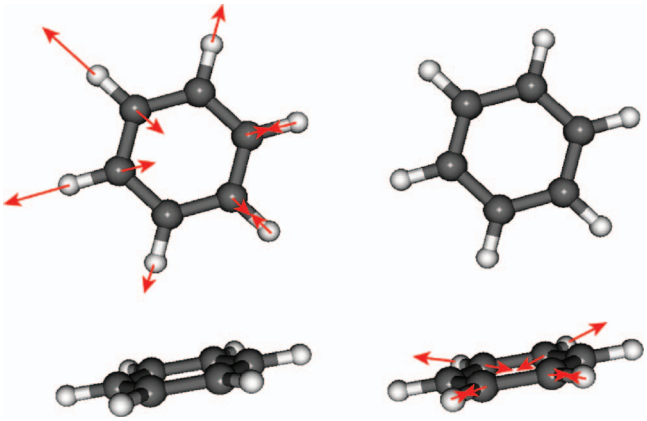

FIG. 5. Vector motions of CH stretching vibration (ν_{20}) of tilted benzene dimer (C_s) calculated at ωB97X-D/6-311++G(3df, 2p) level of theory.

and the normal mode analysis was carried out at ωB97X-D/6-311++G(3df, 2p) level of theory using GAUSSIAN 09 program package.[66] Among the four vector motions of ν_{20} (e_{1u} in benzene monomer), two of them are represented in Fig. 5. The vibrational motions clearly show that the Stem and Top sites independently vibrate. Thus, the calculation also supports the negligible coupling between the vibrations of the Stem and Top site Bz molecules.

D. Time profile of the bath states and VER mechanism of Bz_2

1. Time evolution of the bath states

Figure 6 shows the time evolutions of the broad bands (corresponding to the electronic transitions of the bath modes) of the (a) *hd* and (b) *hh* dimers. The time evolutions of the broad band are not so different between *hd* and *hh*, so that they will relax through a similar VER process. In each panel, the most upper profile was observed by exciting band **b** at $\nu_{UV} = 37600\ cm^{-1}$, while the others were observed by exciting band **a** at $\nu_{UV} = 37\,600$, 37 800, and 38 100 cm^{-1}. The corresponding ν_{UV} energies are marked by arrows in the transient UV spectra of Fig. 3. Since the time profiles between the band **b** and **a** excitations with $\nu_{UV} = 37\,600\ cm^{-1}$ are not so different (the top and the second time profiles in each panel), we mainly focus on the time profiles of the band **a** excitation. All the transient signals reach to maximum intensity at roughly $\Delta t = 300$ ps and then gradually decay. The rise of the intensity is due to population flow from the initial levels into the bath states, and the decay is due to the VP. The IR excitation energy of $\sim$3000 cm^{-1} is much larger than the estimated binding energy of Bz_2, 500–800 cm^{-1}.[16,19,20] In fact, we were able to observe time profile of the Bz fragment as will be discussed in Sec. III E. Here, we discuss the time evolutions of the base states based on Fig. 6.

An important point for Fig. 6 is that the profiles are dependent on probe UV frequencies. For example, the ion signal monitored at $\nu_{UV} = 38\,100\ cm^{-1}$ remains strong even at the delay time of 1800 ps, while the ion signals monitored at $\nu_{UV} = 37\,600$ and 37 800 cm^{-1} decay faster than that monitored at $\nu_{UV} = 38\,100\ cm^{-1}$ in both the *hd* and *hh* dimers. This probe UV energy dependence cannot be explained by a VER model involving a single bath mode,[60,62,63] because the single bath mode model predicts that the profile of the bath mode is independent of the probe UV frequency. There are two possibilities to explain the observed UV energy dependence of the time profiles. First possibility is that the vibrationally excited isomers, (stem)*(top) and (stem)(top)*, independently relax with different time constants in the bath states as well as in

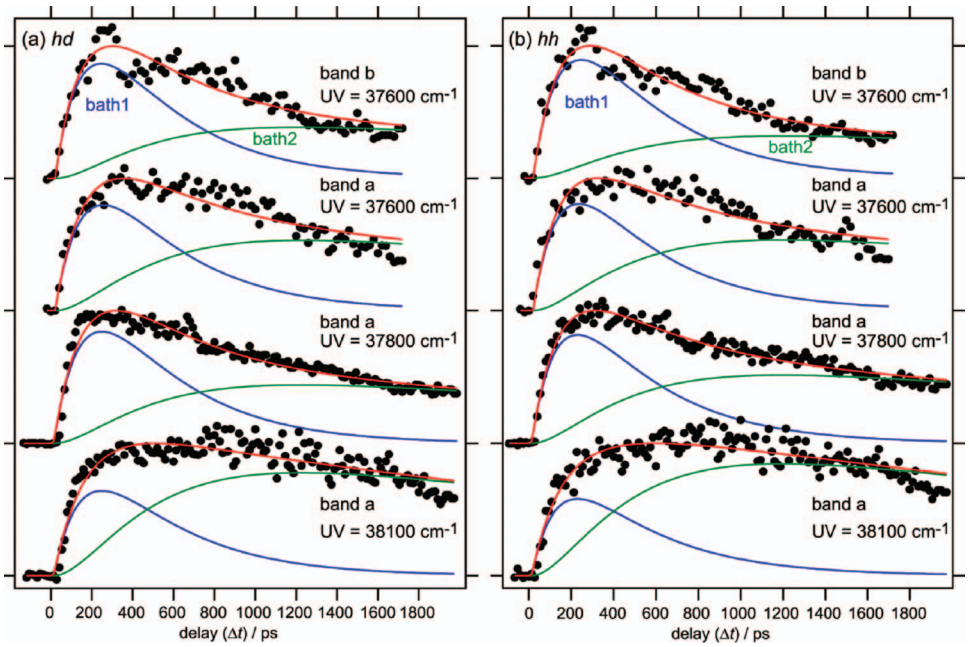

FIG. 6. Time evolutions probed with three different UV energies after the IR excitation of bands **a** and **b**. These were observed by monitoring (a) hd^+ and (b) hh^+ mass channels. Red curves are fitted by using Eq. (2) with $\tau_2 = 400$ and $\tau_{vp} = 4000$ ps. The used τ_1 values correspond to 140 ps for band b. For τ_1 of band a, 150 and 130 ps are used for the *hd* and *hh* dimers, respectively. Blue and green curves represent bath1 and bath2 components, respectively, in each red curve (see text).

the pumped states. The broad transient electronic spectra of the two isomers will appear different from each other. However, this possibility is unlikely because the IR excitation energies ($\sim$3000 cm^{-1}) are much larger than the barrier heights ($< \sim$400 cm^{-1}) for the isomerization to different structures.[54] The vibrationally hot T-shaped dimer having large excess energy will immediately change its structure after the IVR from the initial level. At the bath states, the memory of the Stem and Top site excitation will disappear, and the two isomers will show the same time profile of the bath states.

Second possibility is that the VER process occurs through two bath modes. A schematic diagram of this model is shown in Fig. 1. In this model, the pumped Bz_2 relaxes through the two bath modes (bath1 and bath2) and dissociates as follows:

$$\text{initial} \xrightarrow{k_1} \text{bath1} \xrightarrow{k_2} \text{bath2} \xrightarrow{k_{VP}} \text{fragments}. \quad (1)$$

The time profile of the broad band intensity, $I_{\text{bath}}(\nu_{\text{UV}}, t)$ is expressed by the sum of the intensities of the two bath modes, $I_{\text{bath1}}(t)$ and $I_{\text{bath2}}(t)$,

$$I_{\text{bath}}(\nu_{\text{UV}}, t) = \text{A}(\nu_{\text{UV}})I_{\text{bath1}}(t) + \text{B}(\nu_{\text{UV}})I_{\text{bath2}}(t). \quad (2)$$

Here, $\text{A}(\nu_{\text{UV}})$ and $\text{B}(\nu_{\text{UV}})$ are the absorption cross section of bath1 and bath2, respectively. $I_{\text{bath1}}(t)$ and $I_{\text{bath2}}(t)$ can be described by rate equations of the three-step process, which are also given in supplementary material.[65] On the curve fitting, we used the decay time constant of the Stem site (150 ps) for the rise of the broad band, k_1 ($= 1 / \tau_1$), and fitted by changing k_2, k_{VP}, and the A/B ratio. Red solid curves in Fig. 6 are the best fitted curve with ${k_2}^{-1}$ ($= \tau_2$) = 400 ps, and ${k_{\text{VP}}}^{-1}$ ($= \tau_{\text{VP}}$) = 4000 ps. The components of bath1 and bath2 are represented by blue and green curves, respectively. The fitted curves reproduce well the UV energy dependence, supporting that the two bath modes model can explain the observed VER.

Here, it should be noted that the obtained τ_2 and τ_{vp} values have large uncertainties as shown in Table I. There are two reasons for the large uncertainties: (1) we could not observe the whole time profiles of the broad band until they completely reach to zero because the optical delay line is not long enough to cover whole the time profile, and (2) we used k_1 of the Stem site and neglected the contribution of k_1 of the Top site. In spite of these difficulties, we could reproduce the UV energy dependence on the time profiles in Fig. 6 using the three-step VER model and obtain the time constants for each step. The validity of this model can be further supported by the time profile of the Bz fragment, as shown in Sec. III E. The origins of the two bath modes (bath1 and bath2) will be discussed in Sec. III D 2.

2. Origins of bath states 1 and 2

In the above discussion, we postulated three-step VER model (Eq. (1)) involving bath1 and bath2 states to describe the observed time profiles. This model was originally proposed for the description of VER of the hydrogen-bonded clusters of phenol,[60,62,63] in which "bath1" mainly consists of the high frequency intramolecular modes of the IR excited site and "bath2" consists of the low frequency intermolecular modes. This assignment is based on the result that the relative intensity of bath2/bath1 monitored at higher UV frequency region is larger than that monitored at lower UV frequency. The electronic transitions involving low frequency intermolecular modes are stronger only near the band origin as v'–v'' transitions with $\Delta v \approx 0$, while the transitions involving high frequency intramolecular modes can spread over lower UV frequency region because of the Franck–Condon activities of $\Delta v = -1, -2, -3 \cdots$. This explanation can also be applied to the case of Bz_2. As can be seen in Fig. 6, bath2/bath1 ratio is 1.0 at $\nu_{\text{UV}} = 38100$ cm^{-1} near the origin bands, while it is 0.5 and 0.4 at $\nu_{\text{UV}} = 37\,600$ and 37 800 cm^{-1}, respectively. Thus, similar to the case of the phenol clusters, we can understand that the input IR energy ($\sim$3000 cm^{-1}) in Bz_2 is firstly redistributed within the excited Bz moiety (intramolecular modes, bath1) and is further relaxed to whole the dimer (intermolecular modes, bath2). Vibrationally hot dimer finally shows VP.

E. Time evolution of Bz monomer fragment: VP of Bz_2

The vibrational energy of $\sim$3000 cm^{-1} is much larger than the binding energy of Bz_2, as described above, so that the dimer will finally dissociate via VP. So, we observed the Bz fragment in order to support the proposed model of VER. Figure 7(a) shows the time evolutions of the h^+ and hd^+ ions obtained by exciting the band **a** and monitoring the ion signals at $\nu_{\text{UV}} = 37800$ cm^{-1}. It is obvious that the two profiles are different at long delay time (1200–1800 ps). The h^+ signal is mainly generated via two routes: (1) the ionization of the h fragment generated by VP of the hd and hh dimers in the bath states, and (2) an unavoidable fragmentation of the hh^+ and hd^+ dimer ions after the ionization of the hd and hh dimers. Since bare Bz monomer does not show IVR,[59] it does not give the h^+ signal in the present case. The process (2) provides the

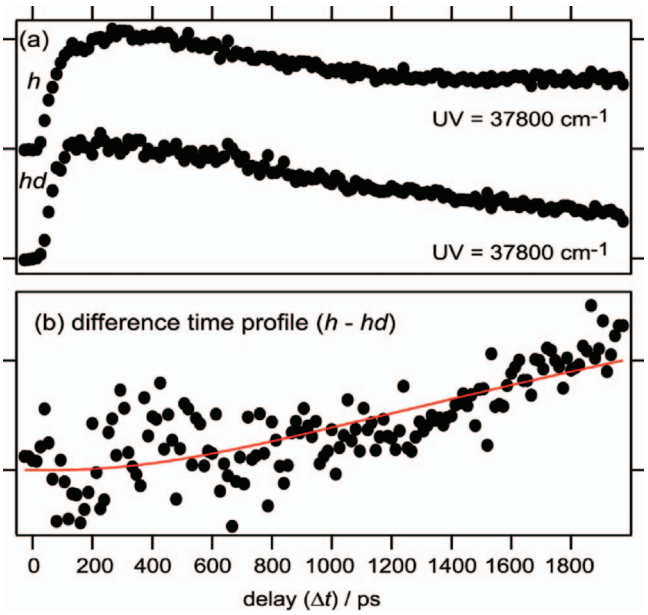

FIG. 7. (a): Time evolutions obtained by monitoring h^+ and hd^+ mass channels with the 37 800 cm^{-1} UV pulse after the IR excitation of band a. (b): A difference time profile subtracting the hd^+ time profile from the h^+ one. Red curve is obtained by a fitting with $\tau_1 = 140$, $\tau_2 = 400$, and $\tau_{\text{vp}} = 4000$ ps.

time evolutions at the bath states of the *hd* and *hh* dimers for the h^+ signal. Thus, the time profile of the h^+ signal consists of the time profile of Bz_2 and that of VP. In order to purely extract the time evolution of the VP process of Bz_2, we subtracted the hd^+ time profile from the h^+ one, both of which are normalized by the intensity at the delay time of 150 ps. Figure 7(b) shows the difference time profile (*h*-*hd*). The signal gradually increases with delay time, so that the difference time profile corresponds to the production time profile of the *h* fragments after VP of Bz_2. The difference time profile can be fitted by the population function of I_{frag} with $\tau_1 = 140$, $\tau_2 = 400$, and $\tau_{vp} = 4000$ ps (red curve),[65] supporting the stepwise VER process of Eq. (1).

F. VER of Bz_3

We extended the pump-probe study to benzene trimer (Bz_3) to examine the size effect on VER. Most of the Bz_3^+ ions dissociate to Bz_2^+ and Bz,[67] so we can observe the pump-probe signal of Bz_3 by monitoring the Bz_2^+ ion. However, the vibrational frequencies are very similar between Bz_2 and Bz_3, which are simultaneously excited by a ps IR laser pulse. The larger contribution of Bz_2 than that of Bz_3 to the Bz_2^+ ion signal makes it difficult to observe the time profile of Bz_3. Fortunately, among the isotopologes of Bz_3 (*hhh*, *hhd*, *hdd*, *ddd*) and Bz_2 (*hh*, *hd*, *dd*), only the *hdd* trimer gives the dd^+ signal after the IR excitation of the CH stretching. Therefore, by detecting the dd^+ signal, we can study VER of the *hdd* trimer. Figure 8 plots time profiles of the dd^+ ion signal after the IR excitation of the CH stretch vibrations. The decay profile of Fig. 8(a) was obtained by fixing the UV frequency at 36 300 cm^{-1}, corresponding to the resonance transition of Bz_3 from band **b**. The signal single-exponentially decays with the lifetime $\tau_1 = 50 \pm 10$ ps. The time profiles of Figs. 8(b) and 8(c) were observed by fixing UV energies at 37 800 and 38 100 cm^{-1}, respectively, corresponding to the time profiles of the bath modes. These time profiles depend on UV frequency used, indicating stepwise VER process similar to Bz_2. By fitting these time evolutions, the time constants were determined to be $\tau_2 = 300 \pm 100$ ps and $\tau_{vp} = 1000 \pm 200$ ps. The smaller error values than those of Bz_2 indicate that other signals do not interfere with the dd^+ signal. From the analogy of the *hd* and *hh* dimers, we can predict that the *hhh* and *hhd* trimers give similar VER time constants.

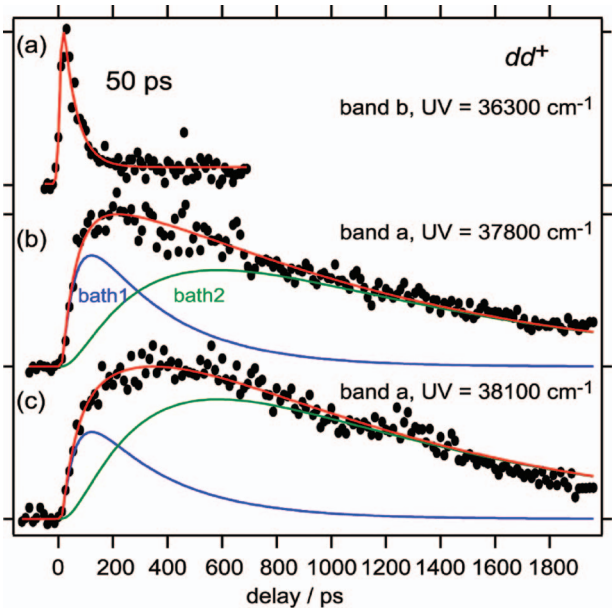

FIG. 8. Time profiles of VER of Bz_3 obtained by monitoring dd^+ signal. Red lines are obtained by fitting with $\tau_1 = 50$, $\tau_2 = 300$, and $\tau_{vp} = 1000$ ps. Blue and green solid lines correspond to bath1 and bath2 time evolutions, respectively.

The shorter IVR lifetime (τ_1) of the *hdd* trimer than that of Bz_2 indicates that the anharmonic coupling between the Fermi-polyad and the intermolecular modes is larger in Bz_3 than that in Bz_2. The faster VP lifetime (τ_{VP}) of Bz_3 than that of Bz_2 can be described by statistical (Rice–Ramsperger–Kassel–Marcus) theory because its time scale is in the nanosecond order. In the theory, the VP rate constant is proportional to the ratio of the total number of possible internal states of the fragment, $W(E_v - E_{diss})$, at the available energy to the density of states of the parent molecule, $\rho(E_v)$, at the vibrational energy. Here E_v is the vibrational energy of the parent cluster and E_{diss} is the dissociation energy. $\rho(E_v)$ of Bz_2 is thought to be higher than that of Bz_3, because Schaeffer *et al.*. reported that Bz_2 has lower frequency intermolecular vibrations than those of Bz_3.[68] On the other hand, $W(E_v - E_{diss})$ of the (Bz_2 + Bz) fragments of Bz_3 will be larger than that of the (Bz + Bz) fragments of Bz_2, when one assumes that the dissociation energy is not so different between Bz_2 and Bz_3. The lower $\rho(E_v)$ and larger $W(E_v - E_{diss})$ of Bz_3 will result in faster VP rate constant of Bz_3 than that of Bz_2.

IV. CONCLUSION

Vibrational energy relaxation of the benzene dimer and timer after the IR excitations of the Fermi polyads of the CH stretching vibration was investigated by picosecond time-resolved IR-UV pump-probe spectroscopy in a supersonic beam. Experiment was carried out using isotopomers, that is Bz-h_6 (*h*) and Bz-d_6 (*d*). Bz_2(*hd*) was used to examine the site difference of the IVR rate constant, and Bz_2(*hh*) was used to investigate the excitation-exchange coupling between the vibrations of the Stem and Top sites in the T-shaped structure. Both *hd* and *hh* dimers gave similar VER dynamics and time constants. The IVR lifetime of the Stem site vibration relaxes ~2.5 times faster than that of the Top site, suggesting a larger "intramolecular mode ↔ intermolecular mode" anharmonic coupling of the Stem site. We also found that the coupling between the vibrations of the Stem and Top sites is very small. The whole VER process is described by three-step energy flow involving two bath modes and the vibrational predissociation. For Bz_3, the VER process also occurs via two bath modes, similar to the case of Bz_2, though the rate constant of each step is faster than Bz_2.

ACKNOWLEDGMENTS

R.K. is supported by JSPS Research Fellowships for Young Scientists. T.E. acknowledges support from the Japan

Society for the Promotion of Science (JSPS) through a Grant-in-Aid project (No. 18205003) and from MEXT through a Grant-in-Aid for the Scientific Research on Priority Area "Molecular Science for Supra Functional Systems" (No. 477). Y.I. thanks the support of the JSPS through a Grant-in-Aid (No. 21350016).

[1]S. K. Burley and G. A. Petsko, Science **229**, 23 (1985).
[2]L. Serrano, M. Bycroft, and A. R. Fersht, J. Mol. Biol. **218**, 465 (1991).
[3]X. Huang, D. F. Shullenberger, and E. C. Long, Biochem. Biophys. Res. Commun. **198**, 712 (1994).
[4]G. B. McGaughey, M. Gagné, and A. K. Rappé, J. Biol. Chem. **273**, 15458 (1998).
[5]M. C. Waters, Curr. Opin. Chem. Biol. **6**, 736 (2002).
[6]L. R. Rutledge, L. S. Campbell-Verduyn, and S. D. Wetmore, Chem. Phys. Lett. **444**, 167 (2007).
[7]V. R. Cooper, T. Thonhauser, A. Puzder, E. Schröder, B. I. Lundqvist, and D. C. Langreth, J. Am. Chem. Soc. **130**, 1304 (2008).
[8]K. C. Janda, J. C. Hemminger, J. S. Winn, S. E. Novick, S. J. Harris, and W. Klemperer, J. Chem. Phys. **63**, 1419 (1975).
[9]J. M. Steed, T. A. Dixon, and W. Klemperer, J. Chem. Phys. **70**, 4940 (1979).
[10]J. B. Hopkins, D. E. Powers, and R. E. Smalley, J. Phys. Chem. **85**, 3739 (1981).
[11]P. R. R. Langridge-Smith, D. V. Brumbaugh, C. A. Haynam, and D. H. Levy, J. Phys. Chem. **85**, 3742 (1981).
[12]K. H. Fung, H. L. Selzle, and E. W. Schlag, J. Phys. Chem. **87**, 5113 (1983).
[13]K. S. Law, M. Schauer, and E. R. Bernstein, J. Chem. Phys. **81**, 4871 (1984).
[14]K. O. Börnsen, H. L. Selzle, and E. W. Schlag, Z. Naturforsch. **39a**, 1255 (1984).
[15]K. O. Börnsen, H. L. Selzle, and E. W. Schlag, J. Chem. Phys. **85**, 1726 (1986).
[16]J. R. Grover, E. A. Walters, and E. T. Hui, J. Phys. Chem. **91**, 3233 (1987).
[17]R. H. Page, Y. R. Shen, and Y. Y. Lee, J. Chem. Phys. **88**, 4621 (1988).
[18]A. Kiermeier, B. Ernstberger, H. J. Neusser, and E. W. Schlag, Z. Phys. D: At., Mol. Clusters **10**, 311 (1988).
[19]A. Kiermeier, B. Ernstberger, H. J. Neusser, and E. W. Schlag, J. Phys. Chem. **92**, 3785 (1988).
[20]H. Krause, B. Ernstberger, and H. J. Neusser, Chem. Phys. Lett. **184**, 411 (1991).
[21]W. Scherzer, O. Krätzschmar, H. L. Selzle, and E. W. Schlag, Z. Naturforsch. **47a**, 1248 (1992).
[22]B. F. Henson, G. V. Hartland, V. A. Venturo, P. M. Felker, J. Chem. Phys. **97**, 2189 (1992).
[23]E. Arunan and H. S. Gutowsky, J. Chem. Phys. **98**, 4294 (1993).
[24]V. A. Venturo and P. M. Felker, J. Chem. Phys. **99**, 748 (1993).
[25]U. Erlekam, M. Frankowski, G. Meijer, and G. von Helden, J. Chem. Phys. **124**, 171101 (2006).
[26]U. Erlekam, M. Frankowski, G. von Helden, and G. Meijer, Phys. Chem. Chem. Phys. **9**, 3786 (2007).
[27]J. A. Odutola, D. L. Alvis, C. W. Curtis, and T. R. Dyke, Mol. Phys. **42**, 267 (1981).
[28]P. Hobza, H. L. Selzle, and E. W. Schlag, J. Chem. Phys. **93**, 5893 (1990).
[29]P. Hobza, H. L. Selzle, and E. W. Schlag, J. Phys. Chem. **97**, 3937 (1993).
[30]P. Hobza, H. L. Selzle, and E. W. Schlag, J. Phys. Chem. **100**, 18790 (1996).
[31]R. L. Jaffe and G. D. Smith, J. Chem. Phys. **105**, 2780 (1996).
[32]V. Špirko, O. Engkvist, P. Soldán, H. L. Selzle, E. W. Schlag, and P. Hobza, J. Chem. Phys. **111**, 572 (1999).
[33]S. Tsuzuki, T. Uchmaru, K. Matsumura, M. Mikami, and K. Tanabe, Chem. Phys. Lett. **319**, 547 (2000).
[34]S. Tsuzuki, T. Uchmaru, K. Sugawara, and M. Mikami, J. Chem. Phys. **117**, 11216 (2002).
[35]S. Tsuzuki, K. Honda, T. Uchimaru, M. Mikami, and K. Tanabe, J. Am. Chem. Soc. **124**, 104 (2002).
[36]M. O. Sinnokrot, E. F. Valeev, and C. D. Sherill, J. Am. Chem. Soc. **124**, 10887 (2002).
[37]M. O. Sinnokrot and C. D. Sherill, J. Phys. Chem. A **108**, 10200 (2004).
[38]R. Schmied and K. K. Lehman, J. Mol. Spectrosc. **226**, 201 (2004).
[39]M. O. Sinnokrot and C. D. Sherrill, J. Am. Chem. Soc. **126**, 7690 (2004).
[40]T. Sato, T. Tsuneda, and K. Hirao, J. Chem. Phys. **123**, 104307 (2005).
[41]A. Heβelmann, G. Gansen, and M. Schütz, J. Chem. Phys. **122**, 014103 (2005).
[42]R. Podeszwa, R. Bukowski, and K. Szalewicz, J. Phys. Chem. A **110**, 10345 (2006).
[43]M. O. Sinnokrot and C. D. Sherrill, J. Phys. Chem. A **110**, 10656 (2006).
[44]T. Rocha-Rinza, L. D. Vico, V. Veryazov, and B. O. Roos, Chem. Phys. Lett. **426**, 268 (2006).
[45]A. Puzder, M. Dion, and D. C. Langreth, J. Chem. Phys. **124**, 164105 (2006).
[46]T. Janowski and P. Pulay, Chem. Phys. Lett. **447**, 27 (2007).
[47]R. A. DiStasio, G. von Helden, R. P. Steele, and M. Head-Gordon, Chem. Phys. Lett. **437**, 277 (2007).
[48]E. C. Lee, D. Kim, P. Jurecka, P. Tarakeshwar, P. Hobza, and K. S. Kim, J. Phys. Chem. A **111**, 3446 (2007).
[49]W. Wang, M. Pitonák, and P. Hobza, ChemPhysChem **8**, 2107 (2007).
[50]E. C. Lee, D. Kim, P. Jurecka, P. Tarakeshwar, P. Hobza, and K. S. Kim, J. Phys. Chem. A **111**, 3446 (2007).
[51]O. Bludsky, M. Rubes, P. Soldan, and P. Nachtigall, J. Chem.Phys. **128**, 114102 (2008).
[52]S. Grimme, C. Mück-Lichtenfeld, and J. Anthony, Phys. Chem. Chem. Phys. **10**, 3327 (2008).
[53]J. Gräfenstein and D. Cremer, J. Chem. Phys. **130**, 124105 (2009).
[54]Ad van der Avoird, R. Podeszwa, K. Szalewicz, C. Leforestier, Rob van Harrevelt, P. R. Bunker, M. Schnell, Gert von Helden, and G. Meijer, Phys. Chem. Chem. Phys. **12**, 8219 (2010).
[55]M. F. Vernon, J. M. Lisy, H. S. Kwok, D. J. Krajnovich, A. Tramer, Y. R. Shen, and Y. T. Lee, J. Phys. Chem. **85**, 3327 (1981).
[56]G. Fischer, Chem. Phys. Lett. **139**, 316 (1987).
[57]R. H. Page, Y. R. Shen, and Y. T. Lee, J. Chem. Phys. **88**, 4621 (1988).
[58]R. Kusaka and T. Ebata, Angew. Chem., Int. Ed. **49**, 6989 (2010).
[59]T. Ebata, M. Kayano, S. Sato, and N. Mikami, J. Phys. Chem. A **105**, 8623 (2001).
[60]M. Kayano, T. Ebata, Y. Yamada, and N. Mikami, J. Chem. Phys. **120**, 7410 (2004).
[61]Y. Yamada, N. Mikami, and T. Ebata, J. Chem. Phys. **121**, 11530 (2004).
[62]Y. Yamada, M. Kayano, N. Mikami, and T. Ebata, J. Phys. Chem. A **110**, 6250 (2006).
[63]Y. Yamada, Y. Katsumoto, and T. Ebata, Phys. Chem. Chem. Phys. **9**, 1170 (2007).
[64]R. H. Page, Y. R. Shen, and Y. T. Lee, J. Chem. Phys. **88**, 5362 (1988).
[65]See supplementary material at http://dx.doi.org/10.1063/1.3676658 for the analysis of quantum beats and rate equations of a three-step process.
[66]M. J. Frisch, G. W. Trucks, H. B. Schlegel *et al.*, GAUSSIAN 09, Revision B.01, Gaussian, Inc., Wallingford, CT, 2010.
[67]T. Iimori, Y. Aoki, and Y. Ohshima, J. Chem. Phys. **117**, 3675 (2002).
[68]M. W. Schaeffer, P. M. Maxton, and P. M. Felker, Chem. Phys. Lett. **224**, 544 (1994).